DRAFT COPY of Nedzved, A., Zalesky B., Ablameyko S., Drozd V., Fridman M. Joint analysis of histological and ultrasonic images to lean state of thyroid gland // Machine GRAPHICS & VISION. vol.16, no 3/4. 2007. pp. 293-304.

A. Nedzved[1)], B. Zalesky[1)], S. Ablameyko[1)], V. Drozd[2)], M. Fridman[3)]

Thyroid gland analysis based on joint processing of histological and ultrasonic images

[1)] United Institute of Informatics Problems of the National Academy of Sciences of Belarus
6, Surganov Str, 220012, Minsk, Belarus
NedzvedA@newman.bas-net.by
[2)] Belarusian Medical Academy of Post-Graduate Education
3, P. Brovki Str., 220013 Minsk, Belarus
[3)] Minsk clinical oncology dispensary.
64 Nezavisimosti av. 220012, Minsk,Belaus
kupriyan@rambler.ru

Abstract

Simultaneous analysis of histological and ultrasonic (US) images of human thyroid glands has been done for thyroid cancer diagnostics. Sizes of follicles were calculated by analysis of distance map for nuclei of cells. Textures on US-images depend on characteristics of follicles. Statistical analysis of US-texture features allows to detect connections of histological and US-images. It was shown that echogenicity of thyroid gland on US imaged depends essentially on size of its follicles. Regions of the organ that contain many follicles of size smaller than size of healthy follicles or contain many destroyed follicles have a low echogenicity. Organ regions that contain many follicles of size considerably greater than size of healthy follicles have low echogenicity, too. This information can be used to avoid surgical procedure, including histological analysis.

1 Introduction

Diagnostics of oncological diseases of internal organs is a complex process that includes several parts [1]. These parts supplement each other but often they are performed separately, since different methods of diagnostics as a rule, are based on different physical, chemical, biological or other principles and, therefore, are carried out by medical experts of different specializations.

Thyroid gland diagnostics traditionally includes such four important steps as ultrasonic examination of the organ [2], cytological and histological tests [3], and the clinical inspection. Ultrasonic diagnostics is one of the most modern ways to detect early morpho-structural changes of thyroid gland. The process of ultrasonic scanning is safe for patients. It can be carried out as required and be repeated many times to provide the case monitoring. The cytological analysis is performed by puncturing thyroid gland (in other words, by excisional biopsy) and following study of cellular structure of obtained tissue of the organ [4]. The cytological analysis is based on the excisional biopsy of the surgically removed organ.

Ultrasonic images (in brief, US-images) are gray-scale pictures that are synthesized by means of reflected ultrasonic waves. Acquisition of those images is based on ability of ultrasound to penetrate inside of the organ and to interact with a tissue. The information about structure and

conditions of the organ is coded via ultrasonic reflected waves. Ultrasonic waves are refracted and reflected mainly at borders of regions, which have different acoustic characteristics. Refracted and reflected waves form a fringe pattern that is usually visible well in US-images. Since changes of conditions of thyroid gland result in variations of acoustic characteristics of regions, US-images of deceased organs differ visibly from pictures of healthy ones. So, the infiltration of tissue, overproduction of colloid, reduction of follicle sizes cause decrease of echogenicity of the organ regions, and growth of the connective tissue or calcification lead to increase of echogenicity. In a case of presence of different pathologic processes thyroid gland can contain regions of increased, normal and lowered acoustic densities [5] that correspond to areas of higher, normal and lower brightness on US-images.

US-images have been used for thyroid cancer diagnostics [6] quite recently. However, ultrasonic diagnostic often allows early detection of cancer and its localization although can not reveal character of tumor. Histological images have been exploited for thyroid cancer diagnostics for a long time [7]. Characteristics extracted from histological images play an important role for final diagnostic conclusions.

Histological images (fig. 1a,4,5) are color images of histological sections photographed with optical magnifications $100 \div 1000$ times. Objects of histological analysis are fragments of a tissue with cells and cellular structures. Because thyroid gland cells fulfill various functions they have different structures, forms and sizes. The average size of healthy nucleus of thyroid gland cells is 5 ± 1.66 microns. Follicles are cellular structures of diameter $10 \div 300$ microns. They consist of colloid surrounded with one or two layers of cells (fig. 1a). Cells and follicles are main objects of healthy thyroid gland while the diseased organ can contain other lumps and structures.

The frequency of ultrasonic waves of a US-scanner does not change during scanning, remaining 7,5MHz or 205,3 microns. The average size of healthy follicles is 70-100 microns while average size of cells is approximately 5 microns. The average size of follicles of the deceased organ can reach 10 microns for the papillary carcinoma and 300-400 microns for the goiter. Deceased follicles change their form from ball-like to prolate and curved. Amount of colloid inside them essentially decreases. In many cases nodes contain completely destroyed follicles. Therefore, it was reasonable to investigate dependence of echogenicity of thyroid gland not only on cell sizes and internuclear scale but also on size of follicles.

Results published by other researchers confirm important role of follicles for vital activity of thyroid gland [6,8]. Efforts of the authors enabled to conclude that echogenicity of nodules and healthy regions of thyroid gland depend on size and conditions of its follicles to a greater extent than on size and conditions of cells.

In this paper, joint analysis of ultrasonic and histological images of thyroid gland is carried out to study dependence of ultrasonic echogenicity of thyroid gland nodules on sizes and conditions of follicles. Information about these characteristics enables to define elements of histological structure of thyroid gland without surgical procedures. To prove this fact, data containing histological and ultrasonic images of 60 patients with verified diagnoses of papillary carcinoma, adenoma and goiter has been used.

2 Ultrasonic images: extraction of thyroid gland features

The analysis of significance of statistics has been done to describe thyroid gland properties. The goal of the analysis was to find statistics and features of ultrasonic images allowing

discrimination of tissues of healthy thyroid gland and deceased thyroid gland without visible changes (nodules, calcifications and other artifacts).

Statistics of three types were used: windowed statistics that are functions of brightness of pixels; statistics on basis of windowed histograms; statistics, which depend on differences of neighbor pixels (that are invariant by global changes of image brightness). Among statistics of the first type windowed moments of different orders and windowed median were calculated. Statistics of the second type were presented by different moments on row mean values of windows and window histograms. The third group of statistics contains central window moments, the Laplace transform $\Delta(\mathbf{I})$ and its windowed average; windowed anisotropy of two types. The anisotropy of first type is a function

$$A_1 = \left|wind(\mathbf{I}) - wind(\mathbf{U}_{\pi/2}\mathbf{I})\right| + \left|wind(\mathbf{I}) - wind(\mathbf{U}_{\pi/2}\mathbf{I})\right| + \left|wind(\mathbf{I}) - wind(\mathbf{U}_{3\pi/2}\mathbf{I})\right|,$$

where the $wind(\mathbf{I})$ means windowed image and the operator $\mathbf{U}_\alpha$ means rotation by the angle α. The second type anisotropy is a statistics

$$A_2 = \left|\nabla_0(\mathbf{I})\right| + \left|\nabla_{\pi/4}(\mathbf{I})\right| + \left|\nabla_{\pi/2}(\mathbf{I})\right| + \left|\nabla_{3\pi/4}(\mathbf{I})\right|,$$

where $\nabla_\alpha(\mathbf{I})$ is the difference derivation in the line having the angle α with the x-coordinate. The "top-hat" transform and windowed filters to extract textures [9] were also used.

It is known that energy of ultrasound reflected by a tissue is an exponentially decreasing function on the depth of penetration inside a body. Investigations have been carried out based on histograms of averaged row brightness to reveal a character of dependence of pixel intensities on depth of ultrasound penetration. They showed lack of decrease of brightness and lack of constant dependence of brightness on depth of penetration of ultrasound inside a tissue at all. The brightness increases on some 2D-images and decreases on others with different velocities. Such effect can be explained by the image correction that is done by modern ultrasonic scanners. As a rule, scanners create US-images performing operations that correct effects of attenuation, absorption and dispersion of ultrasound [10]. However, characteristics of tissues vary with images that result in nonstationarity of image brightness. That is the reason why we paid more attention to statistics of the third type, which depend on differences of neighbor pixels and are affected less by variations of properties of ultrasound.

The initial datasets consisting of 2D slice ultrasonic images of 60 patients with verified diagnosis were used as a learning sample. Only parts of ultrasonic images not affected visibly by some pathological changes were considered for the learning process. Then the stepwise regression and the t-test [11] were used to pick out the most significant statistics in order to separate healthy and deceased tissues. They were the Laplace transform, the anisotropies and one of texture filters. The table of values of those most significant statistics was used to train the LDA, the SVM, and the k-nearest neighbors classifiers with the help of the statistical package **R**. After learning the classifiers were applied to categorize images that were not considered for learning process. The mean values of correctly classified patients amounted $65-70\%$ for each of classes of healthy and deceased patients. At that, results of classification by the SVM [14] and by the k-nearest neighbors classifier [11] coincided for 98% of datasets. The classification via the LDA turned out 3-4% less precise.

To provide a more accurate classification, a joint analysis of histological and US images was done.

DRAFT COPY of Nedzved, A., Zalesky B., Ablameyko S., Drozd V., Fridman M. Joint analysis of histological and ultrasonic images to lean state of thyroid gland // Machine GRAPHICS & VISION. vol.16, no 3/4. 2007. pp. 293-304.

3 Histological images: calculation of internuclear distances and size for follicles.

As described above, thyroid gland features on US-images are formed by cell structures. Therefore, values of nuclear and internuclear distances are the most important characteristics for ultrasonic diagnostics. To estimate influence of cell structures on echogenicity of thyroid gland, an algorithm that computes internuclear distances has been developed. To determine intranuclear distances, the algorithm builds a binary image of nucleus by means of a special segmentation that finds patterns of cell nucleus and marks the rest part of the image as a background. Since usually nucleuses are poorly visible (fig. 1a) the histological image needs enhancement, which is based on peculiarities of its coloring. There are several chemical paint agents. They mark nucleus by red, violet, blue, orange and brawn colors. Hematoxylin-iosin is the most often applied agent that marks nucleus in dark blue and color other image objects in red or leaved them uncolored. Therefore, difference of red and blue channels of the RGB representation of a histological image makes nucleus essentially more contrast (fig.1b). The next step of the algorithm is binarization of the enhanced image by the Otsu threshold segmentation method [12]. After that morphological operations are performed for the binary image consisting of only nucleuses to correct their shapes.

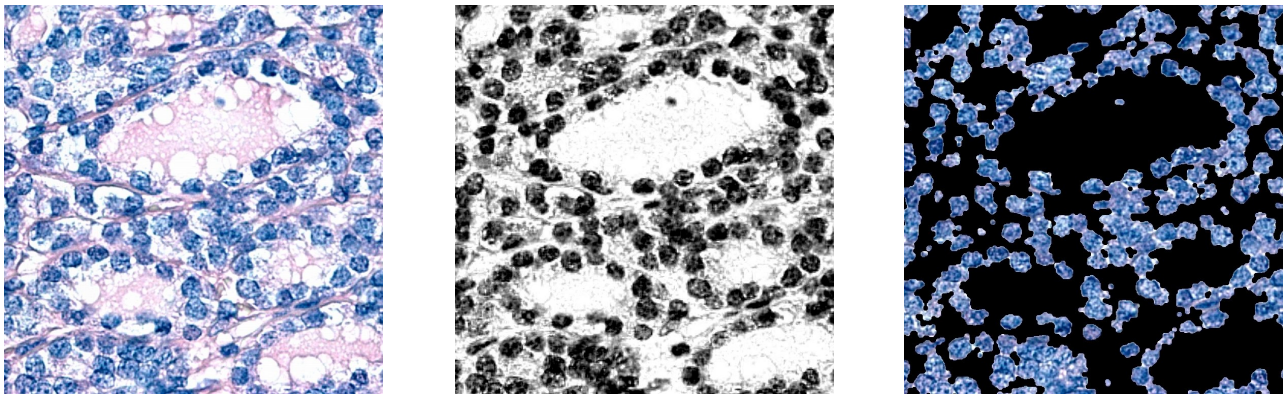

a b c

Fig.1. Steps to exact nucleus patterns from a histological image: a) – original image; b) – enhanced image; c) – image of segmented nucleus

Now the distance map can be computed in order to find the intranuclear distance. Intensity of each pixel of the distance map image corresponds to the distance to nearest nucleus (fig. 2.b).

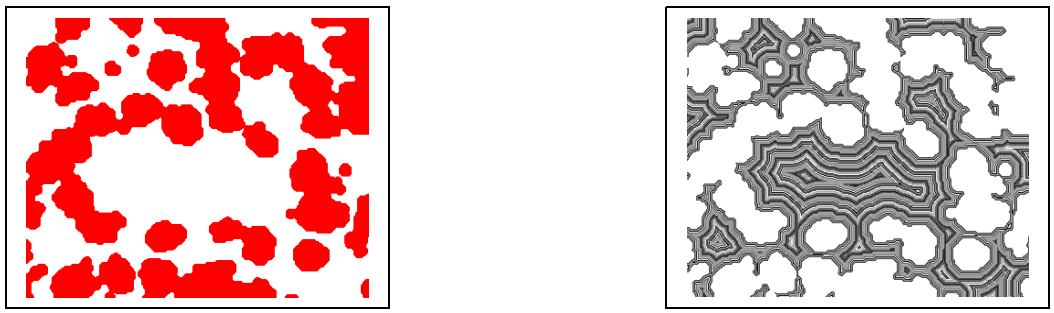

a b

Fig.2. Building the distance map: a) – the original binary image; b) – the distance map.

The Chamfer metrics [13] has been used to build the distance map for its optimality in a sense time/quality. The intranuclear distance was found as a conjunction of the morphological medial lines, which are determined with the help of Chamfer metrics, and the distance map (in this case the traditional morphological thinning gives too large sample of dark pixels that corresponds to incorrect short distances). To find the morphological medial lines, first, pixels corresponding local maxima are found and then the binary thinning is applied to those pixels (fig. 3).

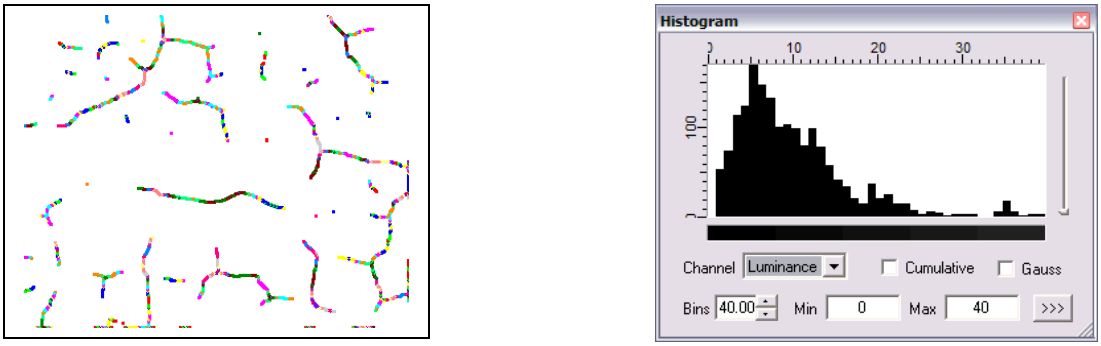

a b

Fig.3. Skeleton image – a) and corresponding histogram of brightness – b).

4 Joint analysis of histologic and US images: Dependence of visible structure on thyroid gland nodes

Two program complexes have been developed to carry out investigations. The program complex "Citron" [15,16] was developed to analyze histological images of different magnifications. It contains a large set of methods for both: investigation of cells and analysis of tissues. "Citron" allows extraction of objects, for instance, cells or their nucleus and some artifacts from histological images; finding a tissue texture and estimation of its topological and geometrical characteristics. As a whole, the complex enables to calculate more than forty characteristics of tissue and cells [17]. The second program complex has been developed to visualize datasets of US-images of large size, containing 100÷ 400 2D-slice pictures of each patient, to segment them, to compute more than 20 their characteristics, to display several local parameters of those, in general, non-homogeneous slides.

To perform the joint analysis of histological and US-images, 32 datasets of patients with two verified diagnosis were used. The first group of pictures consisted of 23 datasets of patients with the diagnosis papillary carcinoma that was verified after removal of the organ. Remaining 9 datasets contained images of patients with the confirmed diagnosis goiter. The dataset of each patient consisted of several color histological images that were acquired by the optical microscope LEICA DMLB2 with magnification x50, x400. Each collection of US-images contains from 100 up to 400 halftone 2D slice pictures of thyroid gland. Average sizes of follicles and sells of 16 patients were computed with the help of the program complex “Citron”. Histological images of 50-fold magnification were used for that since they consisted of the greatest number of follicles visible enough to process them in automatic mode. All measurements of follicle sizes were done inside rectangles of the fixed size. Conditions and sizes of follicles on remaining 16 image datasets were

estimated manually. Those datasets contained histological images that had large areas with strongly damaged follicles (fig.4) or even without follicles filled with other formations. Healthy follicles of the same patient are drawn on fig.5.

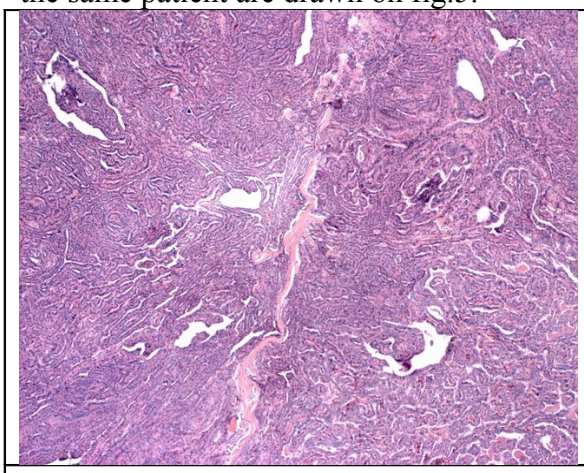

Fig. 4. Histological image sample with deceased follicles

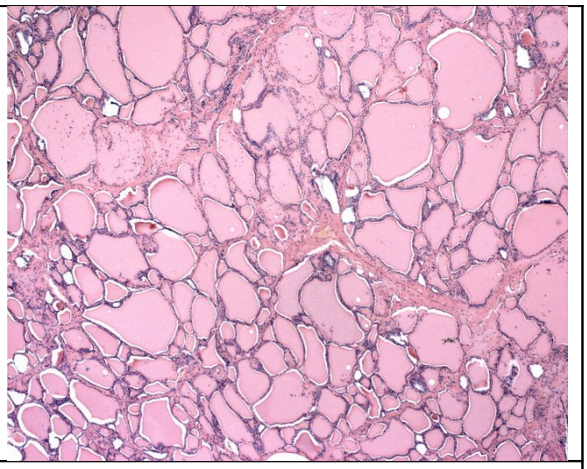

Fig. 5. Histological image of the same patient with healthy follicles

Average sizes of follicles of 16 patients in microns (1mkm=10^{-6}m) adduced in Table 1. They were calculated automatically. Three of these 16 patients had total lack of follicles in areas with pathologies. As we have already mentioned histological pictures of healthy follicles were done for regions of thyroid glands not affected by the diseases. Column means of follicle sizes are written in the last line of the table. Those means are taken over nonzero numbers only. The length of ultrasonic waves of the scanner was approximately equal 205,3 microns.

Dependence of follicle sizes (in a micron) on pathology Table 1

Papillary carcinoma	Transparency of nodules on ultrasound image	Goiter	Transparency of nodules on ultrasound image	Norm	Transparency of nodules on ultrasound image
51,044	texture	310,023	without texture	83,700	texture
30,857	low texture	127,566	without texture	73,767	texture
33,780	low texture	91,749	texture	67,863	texture
53,550	texture	88,890	texture	64,936	texture
11,839	without texture	0	without texture	93,135	texture
25,416	without texture				
80,542	texture				
51,420	low texture				
21,369	low texture				
0	low texture				
0	calcinate				
$\Sigma \approx$ 39,980		$\Sigma \approx$ 154,557		$\Sigma \approx$ 76,680	

The table data allow us to formulate the following hypothesis: the sonolucency (ultrasonic transparency) of deceased regions of thyroid gland on US-images depends more on size and conditions of follicles than on size and state of cells. The argument for this conjecture is the known property of ultrasound to be reflected by boundaries of mediums having different acoustic penetrability [7]. A healthy follicle is a rounded clot of colloid surrounded by the membrane with one or two layers of adjacent cells (fig.1a,5). The size of healthy follicles is $\approx 70 \div 100$ mkm that is between one third and half of the US-wave length. Elementary calculations show that follicles of such magnitude not only move (and if their size is equal half wave length they do not move at all) but also oscillate at their equilibrium positions.

Let us consider follicle of the size $\approx \lambda/2 = 102.65$, where λ is the US-wave length, and let ultrasonic waves be of the form $\sin(2\pi\nu t)$ with the frequency $\nu = c_{us}/\lambda$, where $c_{us} \approx 1540$ m/s is the ultrasound velocity inside a human tissue. Then, if the amplitude of oscillations of the follicle membrane is much less than the length of the ultrasonic wave, the combined wave reflected by both sides of the follicle is of the form

$$r_1 \sin(2\pi\nu t) + r_2 \sin(2\pi\nu (t + \lambda/c)) = (r_1 + r_2)\sin(2\pi\nu t),$$

where $r_1, r_2 > 0$ are cumulative reflectivity factors of sides of the follicle. In this case the reflected signal has the amplitude sufficient to register the US-wave by the scanner receiver. In the case when the distance between the sides of follicle h is not divisible by the half-wave (i.e. $h \neq k\lambda/2$) the amplitude of the reflected signal $A \geq 0$ can be much less than $r_1 + r_2$. For instance, if $h = (2k+1)\lambda/4$, $k = 0,1,2\ldots$ the amplitude of the reflected signal satisfies the estimate $A \leq |r_1 - r_2|$ (here, we should take into account possibility of additional longitudinal oscillation of the follicle).

The mean size of cells of thyroid gland $r_{cell} \approx 5 \pm 1.66$ mkm is approximately 20 times less than the half-wave of ultrasound $\lambda/2$. Propagation of US-wave in a tissue, consisting of cells without follicles, is accompanied by strong absorption and scattering of the signal [7]. It is also confirmed via comparison of histological and US-images. Any thyroid gland nodule with destroyed follicles filled up with cells looks US-transparent despite the fact that the density of cells inside it is much higher than density of cells inside of a healthy tissue.

Oscillations of membranes of healthy follicles, which are induced by emitted US-waves, explain appearance of higher-order reflected harmonics being absent in the emitted signal. The simplest formula of elastic oscillations gives the following form of the reflected wave

$$\varphi(t) = r_1 \sin\{2\pi\nu (t + \theta \sin\{2\pi\nu t\}\} + r_2 \sin\{2\pi\nu (t + 2h/c + \theta \sin\{2\pi\nu (t + 2h/c\})\}, \qquad (1)$$

where the parameter θ depends on the coefficient of elasticity of a follicle membrane and an amplitude of the emitted US-wave. Results of computations of so-called doubled waves, which now are registered by modern US-scanners, are drawn on fig. 7.

Modeling of the function $\varphi(t)$ shows that for follicle size $h = k\lambda/2$ and appropriate values of θ this function contains of harmonics of the second and higher orders. The amplitude of those harmonics is comparable with the amplitude of the emitted waves. This fact agrees well with practice since modern US-scanners register only harmonics of the second order [2].

Fig. 6. Example of 2D ultrasonic image

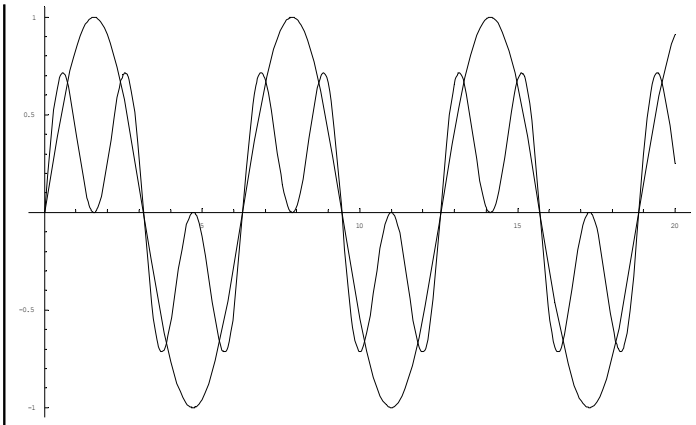

Рис. 7. Doubled wave computed by formula (1).

5 Conclusion

Simultaneous analysis of databases of histological and ultrasonic (US) images of human thyroid glands has been done with the help of two program complexes that had been specially developed for this purpose.

Investigations of histological and US-images of 32 patients (23 of which had papillary carcinoma and 9 had non-malignant growth) revealed dependence of transparency of thyroid gland nodules on conditions of follicles in 31 cases of 32. One case of goiter was not classified satisfactory because the corresponding histological image contains sufficiently large number of undamaged follicles and US-images showed a very large nodule 75% volume of which was textured and approximately 25% turned to be US-transparent.

Note that transparency of thyroid gland nodules can be connected not only with decrease of follicle sizes or their damage. Follicles of the organ affected by goiter can increase in volume 10 or more times. In our datasets follicles expanded many times were observed in 4 cases of 9. On such images areas consisted of expanded follicles alternate with areas containing compressed or even completely destroyed ones. We guess, areas filled up with strongly expanded follicles have increased US-transparency since for linear horizontal resolution of US-scanners ≈ 1 mm each pixel of an US-image contains 12 healthy follicles of average size 80mkm and only 3 deceased follicles of size 300mkm. At that, ultrasound reflects mainly from membranes (in general case, from boundaries of different mediums) and besides elasticity of large membranes varies. These factors definitely affect the frequency and the amplitude of the reflected wave.

It was shown that echogenicity of thyroid gland on US imaged depends essentially on size its follicles. Regions of the organ that contain many follicles of size smaller than size of healthy follicles ($\approx 70 \div 100$ microns) or contain a lot of destroyed follicles have low echogenicity. Regions of the organ that contain many follicles of size considerably greater than size of healthy follicles have low echogenicity, as well.

Acknowledgment

The research was supported by the INTAS 04-77-7036 grant.

Refference

1. Williams E.D., Abrosimov A., Bogdanova T. et al. Guest editorial: two proposals regarding the terminology of thyroid tumors // Int. J. Surg. Pathol.- 2000.- Vol. 8.- P. 181-183.
2. Hopkins C.R., Reading C.C. Thyroid and parathyroid imaging. Semin. Ultrasound CT MR, 1995, 16(4): 279-295.
3. Baloch Z.W., LiVolsi V.A. Follicular-patterned lesions of the thyroid: the bane of the pathologist // Am. J. Surg. Pathol – 2002.- Vol. 117.- P. 143-150.
4. Denham D.W., Angelos P. The pathologist's role in the management of thyroid and parathyroid lesions: the surgeon's perspective // Pathology case reviews. – 2003. – Vol.8, №1. – P.16-21.
5. Maier R. Ultraschalldiagnostik der Schilddruse. N. V.: Schattauer, — 1989.
6. Atkov O. Yu. Basic Trends of Evolution of Ultrasonic Methods of Diagnostics. Visualization in Clinic. № 20, 2002, p. 4-8. .(In Russian)
7. Ablameyko S., Kirillov V., Lagunovsky D. et al. From Cell Image Segmentation to Differential Diagnosis of Thyroid Cancer // Proc. of 16th Intern. Conf. on Pattern Recognition, Aug. 11-15, 2002, Quebec, Canada. – Vol. 1. – P. 763-766.
8. Francoise B.-V. et al. Three-Dimensional Organization of Thyroid Cells into Follicle Structures is a Pivotal Factor in the Control of Sodium/Iodide Symporter Expression. Endocrinology. December 8, 2005 as doi:10.1210. 2005-0805.
9. Forsyth D.A., Ponce J. Computer Vision. A Modern Approach. Prentice Hall. 2003.
10. Webb S. The Physics of Medical Imaging / Taylor & Francis; 1988, P.633
11. Aivazyan S.A., Enukov I.C., Meshalkin L.D. Applied Statistics. Investigation of Dependence. Finansy I Statistika. Moscow. 1985.(In Russian).
12. Sahoo, P.K., Soltani, S., Wong, A.K.C., Chen, Y.C., 1988. A survey of thresholding techniques. Computer Vision, Graphics, and Image processing, 41, pp. 233-260.
13. Gonzalez R.C., Woods R.E. Digital Image Processing. Prentice Hall. 2002.
14. Burges C., A Tutorial on Support Vector Machines for Pattern Recognition, Knowledge Discovery and Data Mining, V. 2.№2, 1998, p. 121–167.
15. Nedzved A.M., Belotserkovsky A.M. The System of Histological Analysis of Oncological Diseases, Proc. 4th Int. Conf. on Information Processing and Control in Extreme Situations, Minsk, Belarus, May 2004, pp.170-176. (in Russian)
16. Nedzved A.,Belotserkovsky A., Ablameyko S. Computer Systems of Histology Images Analysis in Belarus // Annual Proceedings of Medical Sciences – Poland: "Trans Humana" University Press. – Vol.50 S.2, pp 23-25.
17. Belotserkovsky A., Nedzved A., Ablameyko S., Gurevich I., Salvetti O. Automation of Pre-liminary Histological Diagnostics of On-cological Diseases // Proc. on International Conf. on Advanced Information and Telemedicine Technologies for Health (AITTH'2005). – Vol.1. Nov. 8 -10, 2005. - Minsk, Belarus. – P. 70-74

DRAFT COPY of Nedzved, A., Zalesky B., Ablameyko S., Drozd V., Fridman M. Joint analysis of histological and ultrasonic images to lean state of thyroid gland // Machine GRAPHICS & VISION. vol.16, no 3/4. 2007. pp. 293-304.